ANL-6579

Argonne National Laboratory

SURFACE IONIZATION METHOD OF DETECTING HALOGEN-BEARING GASES

by

Harvey A. Schultz

ANL-6579
Instruments
(TID-4500, 17th Ed.)
AEC Research and
Development Report

ARGONNE NATIONAL LABORATORY
9700 South Cass Avenue
Argonne, Illinois

SURFACE IONIZATION METHOD OF DETECTING HALOGEN-BEARING GASES

by

Harvey A. Schultz

Radiological Physics Division

July 1962

Operated by The University of Chicago
under
Contract W-31-109-eng-38

TABLE OF CONTENTS

LIST OF FIGURES

LIST OF TABLES

SURFACE IONIZATION METHOD OF DETECTING HALOGEN-BEARING GASES

by

Harvey A. Schultz

ABSTRACT

In an experimental investigation of positive ion production at heated surfaces, the primary objective was to develop a stable quantitative detector suitable for studies of movements of a gaseous tracer in the atmosphere or other large gaseous masses. Freon-12 (dichlorodifluoromethane) is well qualified as a tracer, since it is harmless to animals, plants, and equipment under ordinary conditions, is undetectable, except by special apparatus, and is not too expensive, considering that 0.1 ppm may be detected. Two phases of the work are discussed: the modification of a commercial detector to improve its reproducibility, and the investigation of the mechanism responsible for halogen sensitivity. A multiple-step process is involved. Steps studied included thermal decomposition of the Freon, release of alkali from a heated source and transfer through the carrier gas to a surface at high temperature, ionization, and ion collection by an electric field. Sensitivity may be lost by raising the halogen concentration enough to make ionization or ion collection the rate-controlling step, and this change is not immediately reversible.

INTRODUCTION

For many years there has been need for an instrument which could be used for the direct study of atmospheric diffusion by means of gaseous tracers. One device on the market, the General Electric Type H Leak detector, met part of the requirements. The purpose of this project was to refine this instrument to meet the demands of the diffusion study.

The term "atmospheric diffusion" used here refers to a process more complicated than gaseous diffusion in the ordinary physical sense. It covers all the mechanisms by which gases from a source, such as a stack, are mixed and diluted in the atmosphere, and includes ordinary diffusion, convection, and effects of the wind. A device suitable for the study of atmospheric diffusion would find additional application in the tracing of gases within enclosures, such as buildings, ducts, and stacks.

The reason for seeking a gaseous tracer was that particles and droplets tend to settle out. Even if the test bodies were so small that settling would be unimportant in isolated tests, the material would accumulate during repeated tests at the same location and be dislodged by air movements or traffic to interfere in later tests.

An ideal tracer would be a gas that is not normally present in the atmosphere and that does not change the properties of the atmosphere. It should be possible to measure its concentration continuously by a portable, relatively inexpensive, piece of equipment with sensitivity so great that the cost of the test gas would not be prohibitive.

Freon-12 (dichlorodifluoromethane), a refrigerant, fulfilled the requirements for a tracer gas because it is odorless, colorless, nontoxic to animals and plants, chemically inert at ordinary temperatures, readily available, and not too expensive to use in view of the great sensitivity of the General Electric Detector. This detector is portable and not too expensive. Other detectors were considered, but this type seemed to be the most promising, although it did give only qualitative indications.

This report covers studies of the commercial detector, of modifications made to it, and of experiments designed to study its mechanism of operation. Much of the material treated here has been available previously, but only in Quarterly and Semiannual progress reports. The results of meteorological field tests have already been published elsewhere, and will not be repeated here.(1)

This paper is divided into 2 major sections. The first covers the commercial detector and improvements. The second covers studies of various processes which take place in such a device, including thermal decomposition of Freon, sensitization of a heated ionizing surface, transportation of gaseous reactants, ionization, and collection of ions.

I. THE COMMERCIAL DETECTOR AND MODIFICATIONS

A. Description of the Type H Leak Detector

The General Electric Type H Freon detector, a compact instrument of simple overall design, consists of a sensing unit, with a pistol grip to be held in the hand, and a cabinet small enough to be suspended from the shoulder. The sensing unit contains the sensitive element and a small fan to pull the air sample through the element. The cabinet contains a power supply and a measuring circuit. The quantity measured is the ionic conductivity between 2 electrodes separated by a thin layer of air at high temperature and atmospheric pressure.

In the sensitive element, the air is drawn through the annular channel between 2 concentric cylindrical electrodes of thin platinum. The inner cylinder, which serves as anode, encloses a heater consisting of a ceramic core wound with a platinum filament. The outer cylinder, which serves as collector, is heated indirectly, by energy transfer across the gap. The outer cylinder is supported only at the ends and is insulated from the surrounding walls by a layer of air. The outer cylinder is 0.7 cm in diameter by 4 cm in length, and the inner is 0.5 mm in diameter by 3 cm, so that the gap is 0.1 cm. The potential difference across the gap is 300 volts. The anode is operated at around 900°C.

This detector responds, with increases in the ion current, to traces of Freon 12 in atmospheric air, in the ppm range. The device is therefore a very effective leak detector. Since the response is not a unique function of the Freon concentration, the original leak detector could not meet the exacting requirements of the problem of atmospheric diffusion.

B. Modification of Equipment and Operating Conditions

The leak detector was developed into a laboratory apparatus suitable for quantitative measurements within the range of Freon concentrations from 0 to 10 ppm. The modified unit eventually used for the published field tests[1] retained from the original equipment only the heater, the anode, and the collector.

The auxiliary equipment was modified first. A strip-chart ion-current recorder and a temperature-control circuit were added, variable collecting potential was provided, and the gas-handling system was improved. The circuit for temperature control utilized a thyratron triggered by a phase-shifting network in which one arm was the temperature-dependent resistance of the platinum heater. The gas-handling system was modified by adding a flowrator and a throttling device, by reducing leaking, and by replacing the fan with a vacuum pump, or, in some cases, by gas under pressure. For mixing special atmospheres, a half-cubic-meter tank was provided.

After these modifications to the auxiliary equipment, the ion current across the air gap was much less erratic than formerly, but it still varied slowly with time. It was found that humidity variations were partly responsible for this slow drift. To eliminate these variations, arrangements were made to reduce the concentration of water vapor to a very low level. For laboratory studies of the equipment, the air could be dried before any Freon was added. For more general applications, it was possible to dry the air with cold traps.

In general, the background ion current (without Freon) diminished throughout the day, whether Freon was added to the air from time to time or not. The rate of this decay was not always the same. In some cases, the rate could be reduced or practically eliminated by adding to the air hydrogen in concentrations of 3 or 4%.

The sensitive element and its enclosure were also modified as the development program continued. A new detector "head" was designed to reduce air leakage, to make it possible to change the material of the collector, and to provide for variable external cooling of this electrode. This head exhibited the best stability yet obtained, but it still did not meet the requirements of the project. Quantitative results became possible under limited conditions. Samples for a number of field tests were analyzed with this equipment.(1)

Other data obtained with this head indicated that Freon sensitivity was the result of a multiple-step process and was not due to a simple reaction. It was concluded that it would be necessary to control each step in order to achieve the desired long-range stability. This led to a different type of investigation, which will be treated in Part II.

II. STUDIES OF THE MECHANISM

An understanding of the mechanism of operation of the General Electric Type H sensitive element was sought in order to be used as the basis for the development of an instrument more suitable for quantitative results. The experimental investigation of the mechanism was started with the commercial detector modified as described in Part I. It was possible to determine the effect of heater temperature, collecting potential, rate of flow, gas composition, time, and collector material. After a combustion furnace had been added to the system, it was also possible to determine the effect of preheating the gas. The results indicated that a multiple-step process was involved. Consequently, special apparatus of several types was built and used in the investigation of particular steps. The objective was to control the entire process by controlling each step. Partial success was attained, as described below.

A. Thermal Decomposition of Freon

Analysts have found that organic fluorides are rather difficult to decompose.(2) One of the reasons for choosing Freon-12 as an atmospheric tracer was its great stability at ordinary temperatures. Evidence that Freon was decomposed in the detector was obtained when the test gas was heated in a quartz combustion tube before being admitted to the modified commercial detector.

The preheating of the gas was part of an unsuccessful attempt to stabilize the net ion current at a "saturation" value corresponding to an integral number of electronic charges per molecule. The number was expected to be 1, 2 or 4, corresponding to one $CCl_2F_2^+$ ion, either 2 Cl^+ ions or 2 F^+ ions, or 2 Cl^+ ions and 2 F^+ ions.

Without Freon, the "background" ion current was found to have the same value whether the air stream was preheated or not. This background increased with temperature in the range from 900 to 1050°C and decreased with increasing rate of air flow in the range from 6 to 180 ml/min (see Fig. 1).

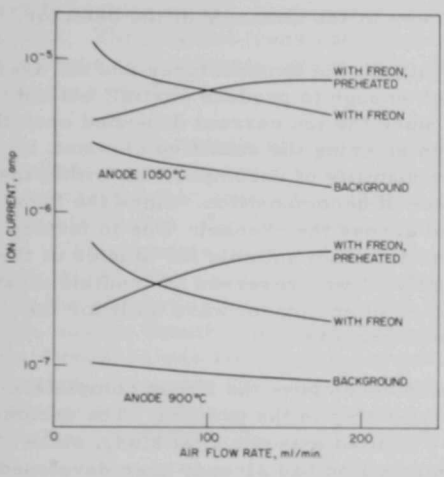

Fig. 1

Effect of temperature, rate of air flow, and preheating of the air-Freon mixture upon the ion current produced in a modified commercial detector. The rate of Freon flow was 8×10^{-5} ml/min, independent of the rate of air flow. To preheat, the gaseous mixture was allowed to flow through a combustion tube before reaching the detector. Tube size was 0.8 cm inside diameter by 30 cm heated length. The temperature was 1000°C.

With Freon introduced into the air stream the ion current depended, in general, upon whether the gas was preheated or not. Without preheating, the net ion current under a constant rate of Freon flow varied in the same direction as background, increasing with increasing temperature and decreasing with increasing rate of air flow. The maximum value of the net ion current was equivalent to 2.7 electronic charges per molecule. This value was obtained at 1050°C and 6 ml/min, respectively the highest temperature then considered safe to this equipment and the lowest flow rate considered to be practical. Preheating the gas in a quartz combustion tube, 0.8 cm in diameter by 30 cm long (heated portion), at 780-1000°C did not improve upon this maximum value of ion current. The net ion current still increased with increasing detector temperature. However, in a series of tests with the furnace at 1000°C the net ion current for constant rate of Freon flow actually increased with increasing rate of air flow, a trend completely opposite to that observed without preheating (see Fig. 1). This indicated that heating of the Freon in the presence of air and quartz produced an outstanding change in the properties of the Freon. In fact, there seemed to be 2 different processes involved, an "activation" and a slower "deactivation," since the effect of the furnace was to increase the ion current if the flow rate was high (180 ml/min), but to decrease it if the flow rate was lower (25 ml/min).

The "activation" was undoubtedly due to the thermal decomposition of Freon to form gaseous products. This conclusion is supported by the literature on halocarbons,[2,3] and also by the results of laboratory tests carried out with combustion tubes at a later time. The undesirable "deactivation" was probably due to the removal of the decomposition products from the air stream, by the walls of the combustion tube or other parts, such as the brass tubing and the screws at the entrance of the detector.

Within the sensitive element itself, the temperatures and the average transit times were normally high enough to produce partial, but not complete, thermal decomposition. Since the ion current depended upon the degree of decomposition of the Freon entering the sensitive element, it must also have depended upon the probability of decomposition within the element, and probably upon the place of decomposition. Since the flow was laminar, the transit time varied across the channel. Due to factors such as these, the detector itself was far from suitable for studies of the mechanism of operation. Consequently, it was reserved for routine measurements, while various special pieces of equipment were built for the study of specific steps of the detection process.

The first step obviously was to decompose the Freon completely before it was made available to the next step in the process. The decomposition step was subjected to only a limited experimental study, since methods suitable for complete decomposition had already been developed.[2] Two different methods were used in preparing gaseous mixtures for experiments on subsequent steps of the detection process. One was to mix the Freon into the air and then pass the mixture through a combustion tube at high temperature to decompose the Freon. Another method, suitable for laboratory studies, was to use chlorine instead of Freon.

The relative effectiveness of different sets of conditions upon the thermal decomposition of Freon were determined by permitting the gas to flow from the combustion tube and to bubble through sodium carbonate solutions, which were then analyzed for the take-up of chlorine. Freon itself passed through undetected.

B. Alkali "Sensitization"

The first detector built entirely at Argonne was sensitive to Freon in only a transient manner. The background ion current, as well as the net ion current due to constant Freon intake, decreased rapidly with time and did not recover. It appeared that some essential factor was missing from this apparatus. It was found that the detector could be resensitized by adding compounds of the alkali metal series. Through subsequent study, many features of the sensitization step have been clarified, but some other features have remained more or less obscure.

1. Alkali in the Furnace-type Unit

In designing the first research detector, the number of different materials was held to a minimum. A straight quartz tube with vertical axis contained 2 platinum electrodes, a wire along the axis and a cylinder covering the inside surface of the tube. A cylindrical electric furnace was used to heat the middle portion of the tube. The test gas flowed vertically upward. The original transient sensitivity was probably due to impurities or surface contaminants, which were subsequently removed gradually from the reaction zone.

The results of 2 investigations suggested that compounds of the alkali metals be tried as the sensitizing agents. One investigation was the spectrographic analysis of samples obtained by washing the surfaces of the electrodes of the modified commercial detector with dilute nitric acid. The elements found and their suspected sources were: Cu from the shell; Al, Si, Mg, Ca, Li, Na, and K for the ceramic heater core; Fe and Ni from the connecting lugs of the collector and Cb, not present in all solutions, source doubtful, possibly from the ceramic. In the other investigation, Freon-12 was admitted to a mass spectrometer. Before it was admitted, a tungsten filament yielded Li, Na, K, and Rb ions. The Freon produced a 20-fold increase in the Li intensity while the other intensities remained essentially the same.

Compounds of the alkali metals lithium, sodium, potassium, and cesium were tried as sensitizing agents in the quartz tube of the furnace-type detector. The materials were added by various methods, including dipping the electrodes into solutions, drawing vapor at high temperature into the detector, and blowing fine particles into it. Nitrates, chlorides, and fluorides were tried. The material in the detector was sometimes redistributed by gaseous discharges in argon, or in mixtures of argon and hydrogen. Treatments of this kind produced an immediate increase in the background ion current and an eventual increase in the absolute Freon sensitivity (i.e., the average number of ions per molecule of Freon). In some cases, Freon sensitivity was completely lacking at first, but developed slowly while the detector was operated. In general, the effects of the sensitization were only temporary. Before long, both the background and the absolute sensitivity decreased continuously with time.

The results of these sensitization experiments left many questions to be answered before stable quantitative Freon detectors could be built. They did not establish where the alkali should be placed for best results, how the sensitivity could be maintained constant for long periods of time, which of the compounds was most effective, or what mechanism was responsible for the sensitization. Partial answers to these problems were sought through a survey of the rather extensive

literature on the ionization of alkalis. Also, information was sought from several organizations outside Argonne. On the basis of the information collected, the experimental attack was continued.

2. Controlled Sensitization

In subsequent experiments upon the sensitization step, the objectives were to explain the mechanism of this step and to develop methods for controlling it without interfering with other essential processes. The approach was to study the effect of the distribution and temperature of alkali compounds upon the stability and halogen sensitivity of laboratory-built detectors and to study, by independent methods, the effect of gaseous halogen compounds upon heated alkali compounds. All this work was carried out in gases at atmospheric pressure.

Based upon the distribution of alkali, all laboratory-built ionization units might be characterized as "directly loaded," "separate-source," or "no-source" models. The directly loaded units were those in which the ionizing surface was coated with alkali-bearing materials. In separate-source units, the ionizing surface was not coated, but alkali was supplied from an auxiliary heated source nearby. In no-source models, no alkali was present, except possibly in regions at low temperature or remote from the ionizing surface.

In the laboratory-built models, the ionization was usually produced at a filament of platinum or of Nichrome (composed of nickel, iron, and chronium) or Chromel A (80 Ni-20 Cr); glass and ceramic surfaces were also tried. The auxiliary alkali source was another filament, or some sort of cup or boat.

The directly loaded surfaces were found to be sources of positive ions at temperatures above about 700°C, but they were insensitive to Freon or its decomposition products. The separate-source units produced ions when both the ionizing surface and the auxiliary source of alkali were heated sufficiently and the ionizing surface was made positive relative to a collecting electrode. Some of these separate-source units were definitely sensitive to gaseous halogen compounds. No-source units gave only low, transient ion currents, as in the case of the furnace-type detector before alkali had been added. Therefore, only the separate-source type of unit was deemed worthy of further investigation.

In designing units to be used in the study of the details of the sensitization process, the source of ionizable material was isolated and an independent temperature-control circuit was provided for it. Two of the designs are shown in Figs 2 and 3. The electrodes were so arranged that vapor from the source was carried a short distance to the filament, by natural or forced convection.

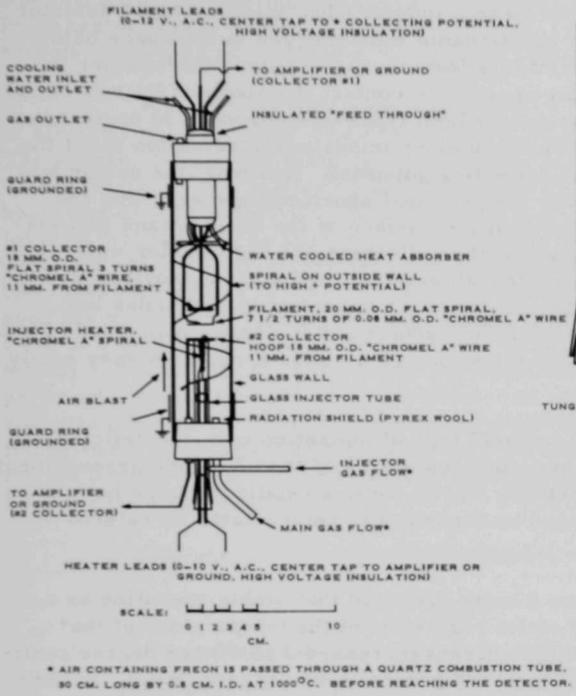

Fig. 2

Injector-type, alkali-sensitized halogen detector (left) and the injector alone.

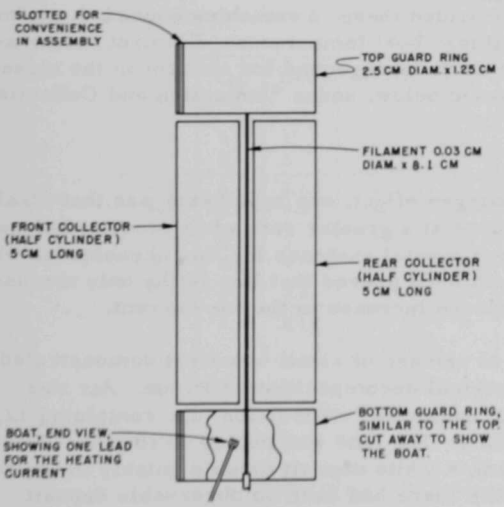

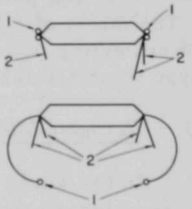

Fig. 3

Electrode arrangement in the closed-vessel unit, and top views of 2 designs of boat. The straight boat was replaced by the C-shaped boat to improve the temperature uniformity. The material was platinum. The current leads are marked (1), the thermocouple and voltage leads (2). The filament was on the side opposite leads (2).

In the earlier of these 2 models, the "injector-type" detector of Fig. 2, two independent gas streams were merged in the space below the filament. The purpose of this feature was to determine whether it was necessary for the halogen gases to contact the alkali at its source, or whether it was only necessary for both types of compounds to contact the ionizing filament. This detector yielded important information about the effects of temperature and collecting potential. However, the design was not completely satisfactory. Its principal shortcomings were that the field strength was not uniform at the surface of the filament and that elevated temperatures prevailed at the collectors and the injector wall, also at the outside envelope, even though external cooling was provided by a vertical air blast. Also, the Chromel A filament appeared under low magnification to have a nonuniform surface and to change with time. Platinum was not used in the flat-spiral design because it deforms very easily after heat treatment.

In the "closed-vessel" type of ionization unit, the deficiencies of the injector type were overcome by means of the electrode arrangement of Fig. 3, with the axis vertical, and by using a relatively large bell as an enclosure. The gas enclosed by the bell was recirculated by natural convection.

Studies of these 2 units indicated that stable operation as a halogen detector required strict regulation of the temperature of the source of alkali, since the ion current increased 2 to 4% per degree centigrade, whether gaseous halogen compounds were present or not. In contrast, the ion current was relatively insensitive to the filament temperature and to the collecting potential, provided these 2 variables exceeded minimum values. The effect of all 3 variables: boat temperature, filament temperature, and collecting potential, upon the background ion current in the closed-vessel type of unit will be discussed below, under "Ionization and Collection."

3. Halogen Effect

In the study of the halogen effect, one hypothesis was that alkali atoms were released from a source at a greater rate when reactive halogen gases were present. Direct experimental evidence for this phenomenon will be presented. However, it has not been proved that this is the only mechanism which will produce a halogen-induced increase in the ion current.

The increased rate of release of alkali was first demonstrated in connection with studies of the thermal decomposition of Freon. Air was passed through a platinum-lined, horizontal combustion tube containing Li_2O formed by decomposition of Li_2CO_3. The tube was heated to 1000°C. With 3% Freon added to the gas stream, a white deposit formed quickly in the cool downstream end of the tube, where there had been no observable deposit

when air without Freon had been used. Both this deposit and the material left in the heated portion of the tube gave positive tests for Li, Cl, and F. It must be noted that the Freon concentrations were very much higher than usual.

A number of quantitative measurements of the rate of release of alkali by chlorine were obtained by Mr. R. G. Hussey and the writer. The source of ionizable material was a boat similar to the C-shaped model used in the bell-type ionization apparatus in Fig. 3. This platinum foil boat, loaded with potassium carbonate, was mounted on a standard taper joint so that it would be positioned near the center of an inverted one-liter spherical flask of dry argon during experimental runs. Flame photometer techniques were used to measure the total amount of potassium deposited upon the walls of the flask. Most of the deposit was inside a circle about 5 cm in diameter, directly above the boat. Boat temperatures of approximately 720°C and 790°C, higher than normally employed in ionization experiments, were chosen so that techniques for sample collection and analysis could be established while using test runs of moderate length. Background (no halogen) experiments gave an energy of activation of 2.1 ev for the overall process. Chlorine was used as the halogen test gas to simplify the experiment.

The results are collected in Table I.

Table I

RELEASE OF POTASSIUM FROM A BOAT BY CHLORINE ADDED TO ARGON ATMOSPHERE

Reaction Conditions			Deposits, % of Ideal[a]			Half-life of Remainder, hr
			During Reaction		Remainder[d]	
Temp, °C	Cl_2, ml[b]	Time, hr	Gross, %	Net,[c] %	Net, %	
720	0.1	1	34	31	21	0.8
720	0.1	2	55	49	2	
791	0.1	0.5	34	26	3	
808	0.1	0.5	34	26	4	
788	0.1	1	37	21	0	
785	0.1	1	34	18	6	
794	0.2	0.5	30	26	48	0.6
27	0.1	0.25	0	0	4 (720°C)	

(a) Ideal deposit calculated at the rate of one K atom per each Cl atom added to the argon.

(b) At atmospheric temperature and pressure.

(c) Net deposit is gross deposit less background (no Cl_2) deposit corresponding to the same temperature and time.

(d) Obtained in argon atmosphere, with no additives.

Chlorine increased the average rate of potassium deposition every time it was used. However, the effect was quite small in the case in which the argon-chlorine mixture was allowed to stand at room temperature (27°C) for 0.25 hr, after which the mixture was replaced with argon alone and the boat was heated to 720°C. The "remainder" column of the table shows only 2 cases in which a substantial net deposit (above background) was obtained by operation in argon alone after the argon-chlorine mixture had been removed.

A complete interpretation of these results cannot be established from the data themselves. Determinations of the chlorine content of the deposits and of the exhaust gas would have been helpful. Some of the chlorine (not over 17% was lost due to the filling of the connecting tubing and due to thermal expansion of the gaseous mixture. If each K atom of the deposit was bonded to one Cl atom, then amounts of Cl_2 ranging up to nearly one-half of the total were left unaccounted for. Possibly these portions were pumped out at the end of the reaction, adsorbed, or taken up in some other manner.

The amount of potassium deposited as KCl was quite likely intermediate between the "gross" and the "net" values of the table. Just 1% of 0.1 ml Cl_2 would have been enough to cover the surface of the material in the boat with a KCl layer 10^3 atoms thick, if the Cl_2 penetrated that deeply. The "remainder" of Table I must have been held over in the boat as either a layer of KCl or a mixture of KCl and K_2CO_3 (or K_2O). It should be noted that the melting point of KCl is 776°C, between the 2 regions used in the experiments. During the "reaction" portion of the experiment, any potassium leaving the boat as K_2CO_3 or K_2O might have reacted with Cl_2 in the vapor phase and then been deposited as KCl. Thus, it was established that chlorine released potassium from a heated boat at an increased rate, but no certain conclusion was drawn as to the details of the process.

C. Mechanics of the Gaseous Medium

Nearly all the ionization experiments were carried out in a gas at atmospheric pressure, since the proposed application of the ionization process was the measurement of the concentration of gaseous tracers in atmospheric air. Aside from any chemical effects the major gas may have had, it served to transfer ionizable material to the ionizing surface, to carry heat away, and to influence the process of ion collection. The transfer of ionizable material was essential to the operation. The other 2 effects were, by comparison, of incidental nature. All 3 processes depended upon the geometrical arrangement of the electrodes as well as upon the properties of the gas. A variety of electrode arrangements was tried, depending upon the materials utilized and the tests that were planned, but no really systematic study of geometrical factors was made. Sources of ionizable material which were "downstream" from the ionizing surface operated satisfactorily in all cases, except one, in which there was a narrow connecting tube, which presumably removed all the ionizable material through condensation upon its walls.

1. Physical Effects of the Major Gas in the Injector-type Unit

The injector-type unit was the first to be built with a separate source of ionizable material under independent control. Most of the parameters studied with this unit were later reinvestigated, under more strictly controlled conditions, with the closed-bell-type unit. However, the basic injector principle, which employed 2 separate channels of flow, was not duplicated in any other unit.

The electrode arrangement is shown in Fig. 2. The source of ionizable material was an electrically heated, alkali-treated spiral heater mounted in the open end of the injector. The tracer gas could be introduced into either the injector channel or the main channel. This detector was supplied with 3 separate ion collectors, which could be used separately or connected in parallel. The ionizing filament was a flat spiral, and the gas flowed perpendicular to its plane. Two collectors were on the side first contacted by the moving gas stream, one on the other side, in parallel planes, each 11 mm from the plane of the filament. The 2 collectors on the first side were the tip of the injector heater and a ring in the main flow channel. The collector on the opposite side of the filament was a flat spiral. This arrangement of collectors made it possible to obtain information about the relative rate of ion production associated with different parts of the filament.

This detector was found to be sensitive to Freon decomposition products (decomposed by passage through a combustion furnace) in either channel so long as the injector heater was on. Sensitivity to these products in the injector channel may be explained as due to an increase in the rate of release of ionizable material, but the reason for sensitivity to decomposition products in the main channel has not been established. The rates of flow were low, usually 30 ml/min in each channel. Under these conditions the average linear velocity in the injector channel was 30 times that in the main channel, so there appears to have been little chance for decomposition products in the main channel to have come into contact with the heater spiral. It was thought that material might have been released from the outside of the injector tube, yet this tube could be removed, washed thoroughly with aqua regia, rinsed with distilled water, dried, and replaced without affecting the sensitivity of the apparatus to Freon decomposition products in the main channel.

If the injector heater was turned off, the background ion current dropped quickly to a very low value and the Freon sensitivity disappeared. On the other hand, if the gas flow through the injector was stopped, the background ion current just decreased to a new stable value, and the relative halogen sensitivity (signal-to-background ratio) increased slightly over the value obtained with equal volumetric rate of flow in both channels. Apparently, ionizable material was being supplied from the injector by diffusion and by natural convection.

The relative rates of ion collection at the 3 collectors were nearly the same whether halogen-bearing gases were present or not. The major portion of the positive-ion current was made up of ions which moved in a direction opposite to the direction of gas flow, to be collected by the injector heater and the concentric ring in the main channel. The exact distribution varied with the conditions of operation, but the 2 collectors below the ionizing filament usually accounted for 70 to 80% of the ion current, indicating that most of the ions were formed on the side of the filament first reached by the gas streams. The ring in the main channel received some 60% or more of the total ion current to the 3 collectors.

2. Physical Effects of the Major Gas in the Closed-vessel-type Unit

Very striking gas-related differences in ion current were observed when a comparison was made between the use of the two noble gases helium and argon as carrier gas in the closed-vessel-type apparatus. Under conditions as nearly identical as possible, the ion current in helium was 5.7 times that in argon. Under the same conditions, the rate of loss of heat from the filament in helium was 3.2 times that in argon. It was thought that these 2 effects might be closely related. However, a study of the possible relation indicated that the heat transfer effect was very probably due to differences in the convection processes in the 2 gases, but that these differences alone could not account for the 5.7-to-1 ratio of ion currents. The ion-current effect appeared to be almost entirely due to differences in the rate of diffusion of ionizable material in the 2 carrier gases.

The closed-vessel-type unit was designed to have a uniform ionizing surface, a uniform electric field at this surface, and a single, controlled, source of ionizable material. The electrodes sketched in Fig. 3 were located near the center of a bell jar, 9 cm in inside diameter by 18 cm high. The unit was built with relatively wide spacings to minimize the possibility that extraneous sources of ionizable material might develop, due to the heating of the collectors, the electrical leads, or the walls of the enclosure. All electrodes were of platinum, which is oxidation resistant and can be obtained as wires and sheets, quite free of alkali except possibly for surface contamination, which can be removed by washing with water and then flaming. Unfortunately, platinum is quite soft after annealing. To keep the vertical filament straight in spite of thermal expansion, the lower end was attached to a flat tungsten spring adjusted so that the tension was very low when the filament was heated. The collectors and guard rings were connected by tungsten wires to Inconel posts which served as supports and electrical leads through the base plate below the bell jar. These 4 Inconel posts and the 2 used for the filament were located on a 6.5-cm-diameter circle concentric with the cross section of the bell jar. The potassium carbonate-loaded boat and its associated parts (electrical leads and supports) were assembled into a unit which fits into a standard taper joint through the base plate.

The conditions of operation, for the results of this section, were: (1) the filament temperature and collecting potential were high enough so that the ion current dropped quickly when the boat-heating current was turned off, and (2) the motions of the gaseous molecules inside the bell were due entirely to random thermal agitation and natural convection. Both gases were processed, at approximately 200 ml/min, through 2 carbon dioxide traps (-78°C), followed by a tube, 1.6 cm in diameter by 20 cm long, filled with small pieces of calcium metal heated to 325°C. The filament was maintained at the same average temperature in the 2 gases (approximately 1300°K), but optical pyrometer measurements indicated that the temperature distributions along the length of the filament were somewhat different.

The dependence of the rate of heat loss upon the gas was observed with various types of ionization equipment, with forced flow as well as with natural convection, and with a variety of pure gases and mixtures. For instance, the power required to maintain the same average temperature at the anode was greater with nitrogen than with argon, and greater still with nitrogen plus hydrogen as an additive. The pair argon and helium was particularly appropriate for study because the heat transfer effects differed greatly.

Standard treatments of natural convection did not seem to be applicable to the case of the closed-bell ionization experiments. In particular, they did not take into account the extremely small radius of the filament, the very large temperature difference between the filament and the gas, and the very high degree of expansion of the gas during the convection process. An attempt to take these features into account, in at least an approximate manner, resulted in the boundary-layer theory of the Appendix. The line of attack was similar to that used by H. B. Squire[4] for the case of a flat vertical wall.

The theory indicated that very simple relations existed between the convection processes in the 2 noble gases when used with the same filament at the same temperature. All the differences in the convection mechanisms in the 2 gases were linked to a single property, the thermal conductivity of the gas at the temperature of the filament (1300°K), which was approximately 8 times as great in helium as in argon. In a horizontal cross section through a given point on the filament, the calculated thickness of the layer of moving gas varied as the cube root of the conductivity, or as 2 to 1, but the maximum velocity was the same in the 2 gases. The indicated heat losses varied as the $\frac{2}{3}$ power of the conductivity, or as 4 to 1. The ratio of the theoretical heat losses agreed reasonably well with experiment, but the actual calculated values were only a little more than half of the experimental values (see Table II). This is not surprising, as some of the assumptions of the theory were rather arbitrary.

Table II

EXPERIMENTAL AND CALCULATED FILAMENT HEAT LOSSES. CLOSED VESSEL UNIT. FILAMENT APPROXIMATELY 1300°K.

	Helium	Argon	Ratio
Total power, experimental	34.6 watts	10.7 watts	3.2
Radiation, calculated	1.5	1.5	1.0
Conduction at ends, estimated	2.0	2.0	1.0
Convection, by difference	31.1	7.2	4.3
Convection, approximate theory	16.1	4.07	4.0
Convection, empirical[a]	2.04	0.71	2.9

[a] Using the relation obtained by Touloukian, Hawkins, and Jakob[5] for vertical cylinders. The values reported in ANL-5755[6] were too high because of a computational error.

A previous exploration of the heat loss problem, described in ANL-5755,[6] contained some errors which will be pointed out. It is now clear that it was incorrect to apply the Touloukian, Hawkins, and Jakob[5] empirical relation for convection along vertical cylinders, since the 2 systems were not dynamically similar. These workers used much larger cylinders, with much smaller temperature differences, in water and ethylene glycol. Their film thicknesses were much smaller than the diameters of the cylinders, and the inertial forces of the gas were much less important than the viscous forces. On the other hand, in the ionization experiments the diameter of the moving plume of gas was very much greater than the diameter of the wire, except for a very short starting section, and the inertial forces were much more important than the viscous forces. It was also incorrect to make a separate calculation for the effect of thermal conduction in the gas, following the method used by Furry, Jones, and Onsager[7] in their theory of thermal diffusion. They worked with very long narrow channels and with small temperature differences, so that convection velocities were very small. In the ionization experiments, the convection velocities were high enough that the only role played by thermal conduction was to transfer heat from the surface of the filament to the gas in the convection current.

The ratio of 5.7 of ion currents in the 2 gases appeared to be much too large to be attributed to the differences in convection velocities and streamline configurations in the 2 gases. Streamlines were traced by combining the boundary-layer theory of the Appendix with an equation for the continuity of mass. The streamline through the center of the boat approached the filament more closely in the case of argon than in helium, but the transit time was less in argon, so that these effects tended to balance out. These approximate calculations neglected the effect of the

boat power, equivalent to 2.5% of the filament power in helium, 4.4% in argon. Also, they neglected a possible retarding effect of the upper guard ring and of the upper portion of the collectors upon the flow process in helium. In spite of the uncertainties, it appeared that the convection process alone could not possibly be the principal cause of the gas-related ion-current effect.

Diffusion processes in the 2 gases remain to be considered. Just above the surface of the material in the boat the concentration of gaseous ionizable material corresponded to the vapor pressure of the material, and therefore depended upon the temperature but not upon the carrier gas. Material from this region diffused into the moving gas stream and continued to spread outward by diffusion as it was carried upward by convection. To estimate the ratio of the diffusion rates in the 2 gases, argon in helium and argon in argon were taken as models, and diffusion coefficients were calculated on the basis of classical collision theory, assuming Lennard-Jones intermolecular potential functions.[8] The ratio was 4.0 in helium to 1 in argon at the same temperature. However, the temperatures would actually be the same in the 2 gases only at the boat, at the filament, and outside the plume of moving gas. Elsewhere, the temperature would be higher in the case of helium, and this would increase the effective ratio of the diffusion rates above 4.0 to 1. To estimate a practical upper bound for the ratio, diffusion constants were calculated, on the basis of the same model, for points lying on the streamlines through the center of the boat and between the horizontal planes defined by the ends of the collectors. The ratio of the average coefficients was 6.9 to 1.

The exact nature of the ionizable material has not been determined. Argon was used as the model because it is one mass unit above potassium in the periodic table. If the material had not been decomposed at all and had vaporized as potassium carbonate molecules (mass 138), xenon (131) would probably be a more appropriate model, and the above ratios would each be raised by about 20%.

On the basis of this analysis, the ion current ratio of 5.7 may be regarded as composed of 2 factors, 4.0 and 1.43, if the argon model is used. The larger factor accounts for the higher rate of diffusion of ionizable material into the moving helium and through it, at constant temperature. The smaller factor, near unity, represents the combined effects of the differences in temperature and velocity distributions associated with natural convection in the 2 gases.

D. Ionization and the Collection of Ions

Ionization and the collection of the ions are 2 distinct steps in the mechanism of the halogen-sensitive positive-ion apparatus, but they

are so closely interrelated that they will be treated in the same section. To promote the 2 steps, 3 features are required: (1) a suitably located source of ionizable material, (2) a surface at high temperature, and (3) an electric field for ion collection.

For the discussion of ion-current effects, the currents may be divided into 3 classes depending upon the nature of their origin: (1) residual backgrounds, obtained when the regular source of ionizable material is not heated directly, (2) backgrounds, obtained when the regular source is heated directly, but no gaseous chlorine compounds are used, and (3) chlorine-induced ion currents.

The effects of temperature and of collecting potential upon ion currents were studied with various types of emission apparatus, starting with the commercial unit. In this unit, and in some of its successors as well, the anode, the collector, and the gas between them were heated, so it was not possible to determine by varying the collecting potential whether the ions were predominantly positive or negative or whether equal numbers of each were produced by ionization in the interelectrode space. In later units, only one electrode was heated, and it was found that the ion current was due to positive ions formed at the surface of the heated anode. In addition, it was found that some of the transient ion-current effects observed in the early apparatus were due to adsorption of ionizable material upon the anode.

A set of experiments made with a straight platinum filament and a concentric cylindrical collector in dry air in a closed bell (see Fig. 3) will be described, to illustrate the effect of filament temperature, collecting potential, rate of supply of ionizable material, and time upon the background ion current. This work was done with the straight boat (see Fig. 3) before the C-shaped design was developed. The boat was charged with a small piece of potassium carbonate, a portion of a solid formed by melting a quantity of the powdered material in a platinum spoon by means of an air-gas flame, then allowing the liquid to solidify.

1. General Description of Results with the Closed-vessel Unit

Experimental results obtained at a constant boat temperature (555°C) were summarized by a 3-dimensional model (see Fig. 4) constructed to represent the dependence of background ion current upon filament temperature and collecting potential. Each of the vertical cards was cut to represent a curve obtained by experiment. The entire assemblage of data might be represented by a curved surface covering the 3 sides of the model which are visible in the photograph. A general description of the results will be given first; explanations will be offered later.

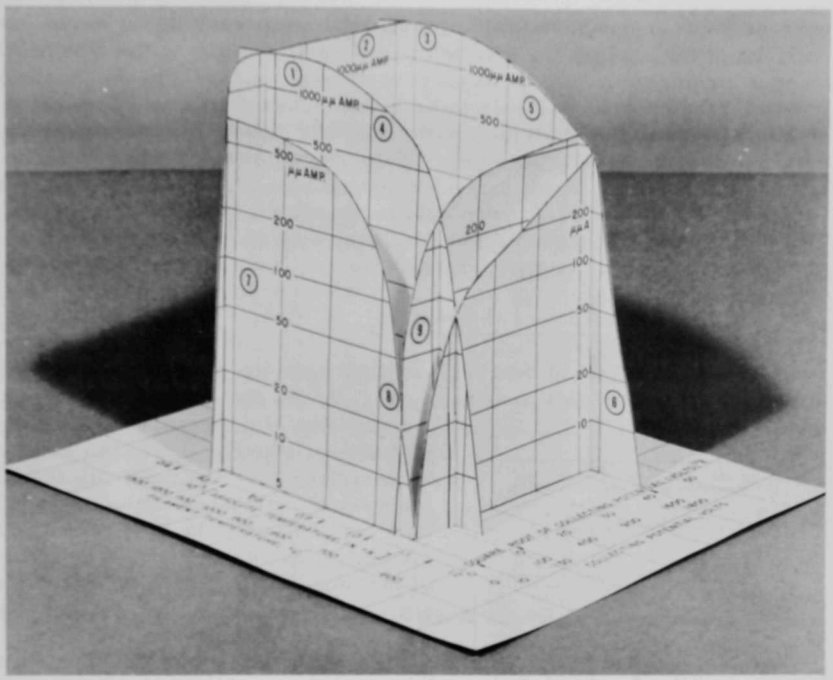

Fig. 4. Positive-ion current (upward) as a function of filament temperatures and collecting potential at a constant boat temperature of 555°C, with dry air in the closed-vessel unit.

It will be noted that the coordinates of the model are the logarithm of the ion current, increasing vertically upward, 10^3 times the reciprocal of the absolute temperature of the filament, and the square root of the collecting potential, each of these increasing from left to right in the photograph. Centigrade temperatures, increasing toward the left, are also shown on a nonlinear scale.

At the top of the model, above numbers 1, 2 and 3, the surface representing the data would lie very nearly parallel to the base of the model, since the ion current was essentially independent of the collecting potential and of the filament temperature as well. To the right of this region, above the numbers 4 and 5, the ion current depended somewhat upon the filament temperature but very little upon the collecting potential. The ion current also varied somewhat with time, approaching the equilibrium values (plotted) by increasing rather slowly after the temperature had been changed. If the boat was turned off after operation in this region, ions were emitted at a decreased rate for a period of time afterward, indicating that some ionizable material had been "stored." In the regions of the surface so far discussed (adjacent to 1, 2, 3 and 4, 5), the ion

current would increase with increasing boat temperature, but in the lower portions of the surface the boat temperature affected only the rate at which an equilibrium value of the ion current was approached. In the region in front of 7 the current was said to be "space-charge limited." It varied with collecting potential and slightly with time, but it did not vary with filament temperature or boat temperature. In the region of the surface in front of 8, 9, and 6, the ion current depended upon filament temperature, collecting potential, and time, but not upon boat temperature. Throughout the entire lower portion of the surface, from 7 all the way around to 6, ionizable material was stored during operation.

2. Effect of Boat Temperature

The effect of boat temperature upon the background ion current in the closed-vessel unit is shown by Fig. 5. As noted there, this graph is a composite of the results of a number of different experiments. The solid curve summarizes data obtained with the filament temperature and collecting potential both high enough to be on a "saturation" plateau, such as found at the extreme top of the model of Fig. 4. The dotted line HB shows a slight space-charge effect, as at the far left upper corner of the model, while JD shows the effect of too low a filament temperature for the rate of delivery of material, corresponding to the far right front portion of the model. The background ion current varied with boat temperature very much like a vapor pressure. The energy of activation of the boat effect was 1.1 ev up to about 600°C, then it increased, becoming 2.0 ev in the 700-750°C range. The reason for this change is not known. Any water of crystallization should have gone off at a much lower temperature, and only very slight decomposition of K_2CO_3 into K_2O and CO_2 takes place at the temperatures involved. (The melting point of K_2CO_3 is 891°C. The flame photometer measurments on the rate of vaporization without chlorine, described above, gave an energy of activation of 2.1 ev for the temperature range 720-790°C.

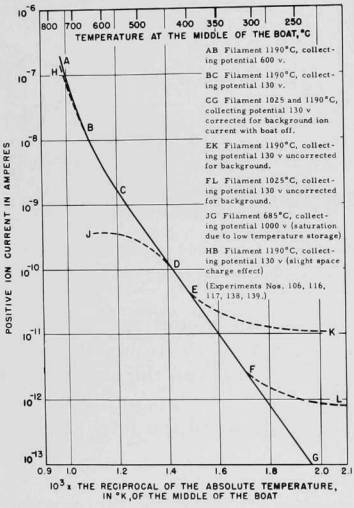

Fig. 5. Effect of the temperature of the boat upon the ion current with dry air in the closed vessel unit.

3. Effect of Collecting Potential

The effect of collecting potential in the closed-vessel unit is plotted in Figs. 6 and 7 for several combinations of boat temperature and filament temperature.

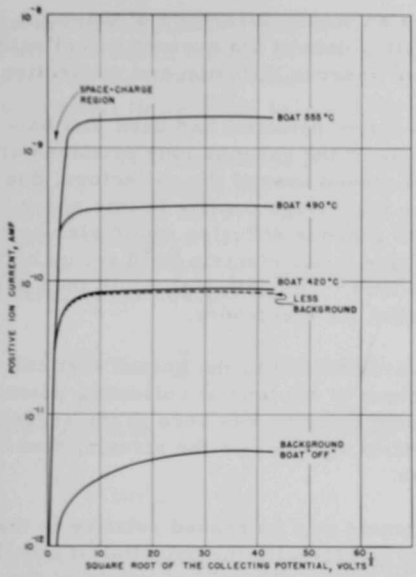

Fig. 6. Ion current as a function of collecting potential at a high filament temperature (1190°C), with dry air in the closed vessel unit.

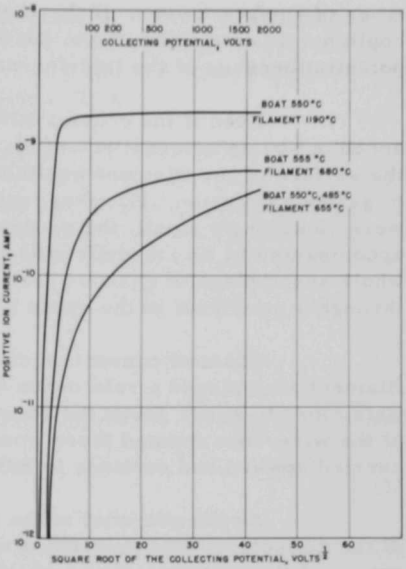

Fig. 7. Effect of collecting potential and filament temperature upon ion current at constant boat temperature, with dry air in the closed vessel unit.

No detectable ion currents ($<10^{-13}$ amp) were obtained when the filament was made negative. This indicated that essentially all the ions collected either arose at the electrodes or were secondaries produced by such ions. Electronic emission at the collector could be ruled out because of the low temperature (near room temperature) and the low electric field (310 volts/cm, maximum) adjacent to its surface. Secondary ionization was very improbable, since the energy gained by an ion from the field was dissipated through frequent collision with molecules of the air at atmospheric pressure.

Filament Temperature at 1460°K. The collecting-potential effects at the highest filament temperature (1460°K) are summarized in Fig. 6.

If all the electrodes were brought to the same potential by external connections, the motions of positive ions produced at the filament and at the boat would depend upon (1) contact potential, (2) gaseous diffusion, and (3) gaseous convection. It might at first appear that the contact difference of potential would have been zero because the electrodes were all of platinum. However, this was not necessarily true, since the filament and the collector were at different temperatures and may have had different

types of surface layers. If there were a contact difference of potential, it could not be determined from the existing data of ion current vs collecting potential because of the interference of gaseous diffusion and convection.

Even if the contact difference of potential had been just balanced out by an external potential, some of the gaseous ions produced at the surface of the filament would have moved toward the collectors, due to gaseous diffusion. However, unless the charge density in this space were vanishingly small, the process of gaseous diffusion would also be accompanied by an ion-drift process, due to the electric field set up by the whole assemblage of gaseous positive ions. The potential would then pass through a maximum in the space between the electrodes.

Gaseous convection currents parallel to the heated vertical filament also played a role in the motions of the ions at collecting potentials close to zero. Since the convection velocity was zero at the surface of the wire, ions formed there would first diffuse into the stream, then be carried upward and continue to diffuse.

As the potential of the filament was increased relative to that of the collectors, the ion current rose steeply with the potential at small values of the potential, then levelled off rather abruptly at values of the ion current which depended upon the boat temperature. At points of the steep part of the curve in Fig. 6, the ion current did not increase when the boat temperature was increased. Also, the ion current did not drop at once to the "boat-off" value when the boat-heating current was turned off, but continued at elevated values for a period ranging from a few minutes to many hours, depending upon specific conditions. In some experiments of short duration, the charge recovery during this period was nearly perfect, as judged by the actual ion current and the saturation value at the same boat temperature. In experiments of longer term the recovery was less efficient.

The high rate of increase of ion current with collecting potential at small collecting potentials (see Fig. 6) appears to have been due primarily to a decrease in the rate of diffusion of gaseous ions back to the filament. The small electric fields near the filament would not have had any significant effect upon the probability of ionization at the surface. This effect will be discussed later.

The lower portion of the family of experimental curves in Fig. 6 agrees quite well with the prediction of an old, simple theory of ion collection in a gaseous medium. The development below follows Thomsons' Conduction of Electricity Through Gases, Third Edition,(9) but uses cylindrical coordinates in place of Cartesian coordinates. The basic assumptions are: (1) gaseous ions are emitted at the filament at a constant rate, independent of the external electric field, (2) gaseous ions

adjacent to the filament are in thermal equilibrium with the neutral gas, (3) all ions which collide with the filament are neutralized, and (4) the ion current in the interelectrode space is entirely due to a radial drift velocity proportional to the local value of the electric field.

The electrodes are 2 long coaxial cylinders of radii a and b with $a < b$. The inner one is the emitter of positive ions and has the higher potential. In the interelectrode space, the electrostatic potential V and the positive charge per unit volume, ρ, are related to the radial distance r from the axis of the cylinders through 2 differential equations: Poisson's equation of electrostatics,

$$\nabla^2 V = \frac{1}{r}\frac{d}{dr}\left(r\frac{dV}{dr}\right) = -4\pi\rho \quad , \tag{1}$$

and an equation for the steady-state current due to the outward drift of ions,

$$i = 2\pi r \rho \mu \left(-\frac{dV}{dr}\right) \quad , \tag{2}$$

in which i is the current per unit length of the filament (independent of r), μ is the ion mobility, assumed to be a constant, and all electrical quantities are expressed in absolute electrostatic units to be consistent with the constant 4π used in Poisson's equation.

Elimination of ρ from the 2 differential equations yields

$$\left(r\frac{dV}{dr}\right)\frac{d}{dr}\left(r\frac{dV}{dr}\right) = \frac{2i}{\mu} r \quad , \tag{3}$$

which may be integrated in two steps. The first integral,

$$\left(r\frac{dV}{dr}\right)^2 = \frac{2i}{\mu} r^2 + \text{constant} \tag{4}$$

may be rewritten as

$$-\frac{dV}{dr} = \left(\frac{2i}{\mu}\right)^{1/2} \frac{(r^2 - \beta^2)^{1/2}}{r} \tag{5a}$$

or as

$$-\frac{dV}{dr} = \left(\frac{2i}{\mu}\right)^{1/2} \frac{(\gamma^2 + r^2)^{1/2}}{r} \quad , \tag{5b}$$

depending upon the sign of the constant of integration. The quantities β^2, γ^2, $(2i/\mu)^{1/2}$, $(r^2 - \beta^2)^{1/2}$, and $(\gamma^2 + r^2)^{1/2}$ are all taken as positive (or zero). A negative sign is chosen on the left-hand side of equations 5a and 5b because the inner electrode was assumed to have the higher potential.

The second integrals are given in most tables, or they may be derived by changing the variables. They may be written as

$$V(r) - V(b) = \left(\frac{2i}{\mu}\right)^{1/2} [f(b) - f(r)] \quad , \tag{6}$$

in which $V(b)$ is the potential at the outer electrode ($r = b$) and $f(r)$ is given by

$$f(r) = (r^2 - \beta^2)^{1/2} - \beta \cos^{-1} (\beta/r) \tag{7a}$$

or

$$f(r) = (\gamma^2 + r^2)^{1/2} - \gamma \ln \frac{\gamma + (\gamma^2 + r^2)^{1/2}}{r} \quad . \tag{7b}$$

According to convention, β and γ are positive (or zero) and $\cos^{-1} (\beta/r)$ is in the first quadrant.

Two boundary conditions are required. One is very simple: let

$$V = 0 \qquad \text{at} \qquad r = b \quad . \tag{8}$$

The other is based upon a relation from the kinetic theory of gases. If there are n particles of a particular kind per unit volume of gas near a surface and their root-mean-square (rms) velocity of agitation is C, then $nC/(6\pi)^{1/2}$ such particles will strike unit area of the surface per unit time. If these particles are positive ions near the filament and if each carries a charge e back to the filament, the current due to this backward diffusion will be $neC/(6\pi)^{1/2}$, in which ne is just the charge density near the filament, ρ_1. Accordingly, the second boundary condition may be written as

$$2\pi a \ \rho_1 C/(6\pi)^{1/2} = I - i \quad , \tag{9}$$

in which I represents the gross rate of emission per unit length of the filament. Combining this with the first integrals (equations 5a and 5b) and the second of the original differential equations (2), all evaluated at $r = a$, the radius of the inner electrode, one obtains

$$\beta^2 = -\gamma^2 = a^2 \left(1 - \frac{C^2}{12\pi\mu} \frac{i}{(I - i)^2}\right) \quad . \tag{10}$$

It is clear that the β form of the solution will be applicable near i = 0, and the γ form near i = I; the two forms agree when $\beta = \gamma = 0$.

Since a << b in the experimental set up ($a/b = 1.15 \times 10^{-2}$), $\beta << b$ for all β and the relation between the ion current and the potential at r = a may be reduced to

$$V(a) = (2i/\mu)^{1/2}\, b \quad . \tag{11}$$

The same equation is also applicable for the lower currents in the γ range so long as $\gamma << b$. When the data of the uppermost curve of Fig. 6 and 7 were replotted as $i^{1/2}$ vs V(a), the result was very nearly linear up to the sharp bend of Figs. 6 and 7 (above 17 volts). To determine a value for the mobility μ, a straight line was drawn through the higher voltage points (7 to 15 volts, 0.3 to 1.2×10^{-9} amp), assuming that small deviations at lower voltages were due to forward diffusion and convection effects. This line gave a mobility of 2.6 cm^2/volt-sec and an apparent contact difference of potential of 1.8 volts to be added to the externally applied potential. This calculated mobility is of the same order of magnitude as published values for relatively large ions in a gas at atmospheric pressure. In fact, it is quite close to the value 2.7 cm^2/volt-sec given for K^+ in N_2 by the American Institute of Physics Handbook.[10] Simple estimates of the effect of forward diffusion and of convection in the range from 7 to 15 volts indicated that each of these was small relative to the mobility effect, but not negligible. They would be expected to affect the ion current in opposite directions.

Due to the geometrical arrangement of the electrodes, (a << b), the values of I, C, and a did not enter explicitly into the determination of the mobility. This was fortunate, as the value of I was not known. It was not given by the high-current asymptote of the uppermost curve of Figs. 6 and 7, since experience has shown that an increase of the boat temperature would give a higher asymptote, but would not change the lower part of the curve. Since I was defined as the gross rate of emission, each ion was to be counted each time it was emitted, independent of whether the same atom had been ionized at the filament one or more times before. It is possible that the assumptions made at the outset of the theory might have been relaxed somewhat without affecting the above calculation of mobility. For instance, it might have been assumed that a fraction of the ions which returned to the filament were reflected, while the remainder were neutralized.

Along the nearly horizontal portions of the collecting-potential curves obtained at a filament temperature of 1460°K, the ion current was controlled primarily by the rate of supply of ionizable material. The slight increase of ion current with voltage was attributed to a decrease in the effect of vertical convection currents.

At Lower Filament Temperatures. Under the conditions of low filament temperatures and relatively high boat temperature, represented by the lower 2 curves of Fig. 7 and the segment JD of Fig. 5, the ion currents exhibited transients which settled down to values that were independent of the boat temperature at all collecting potentials, even the very high ones. These equilibrium values of ion current were lower than the rate-of-supply-limited values just discussed. At least part of the ionizable material which was supplied to the filament but not collected as ions was deposited upon the filament and could be ionized subsequently. The amount thus recoverable increased with time, even after the ion current transients had disappeared. The equilibrium ion currents varied with the filament temperature according to the steep line of Fig. 8, indicating that the rate-controlling step was associated with the filament; the energy of activation was 4.2 ev. The nature of the 4.2-ev step remains unknown. Also, the exact nature of the deposit upon the filament is not known. It may have been in a form different from either the original material in the boat or the material deposited upon the filament by back diffusion under high-filament-temperature, low-field conditions. The average energy required to remove an ion from the surface is nearly the same as that 4.340 ev, required to ionize a gaseous potassium atom. Therefore, if the simple assumptions are made that the particles on the surface are adsorbed potassium atoms, and that the ions are potassium ions, then a Born-Haber type of cycle indicates that the heat of adsorption is nearly the same as the electronic work function of the surface.

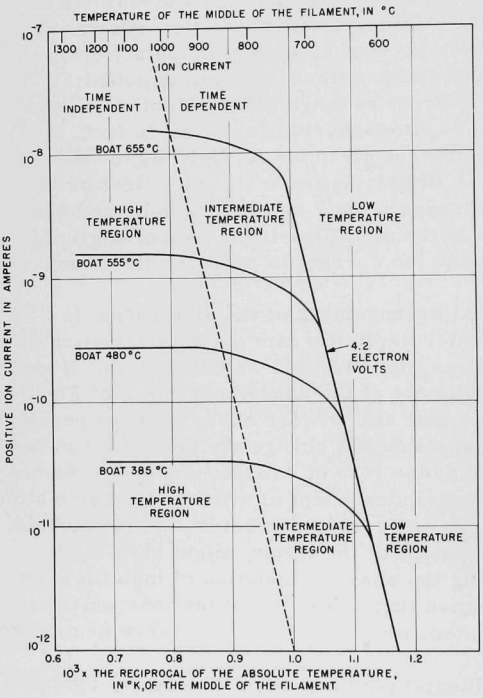

Fig. 8. Effect of filament temperature on ion current at four boat temperatures and a collecting potential of 130 v, with dry air in the closed vessel unit.

The collecting-potential curves obtained at low filament temperatures do not have any segment which agrees with the theory of ion collection discussed above. It appears that forward diffusion and gaseous convection produce the deviations at low voltages, and that the theory breaks down at higher voltages because the

drift velocities of the ions are no longer very small relative to the random thermal velocities. At the higher drift velocities, the ion mobility is not a constant, but varies with the field,[11] and, in addition, the rate of back diffusion is not given by simple gas kinetics. Also, the higher voltages may increase the rate of ionization by lowering the potential barrier that must be crossed as an ion is emitted.

The enhancement of the rate of surface ionization by an external electric field was first discussed by Schottky,[12] and the effect has been associated with his name. He assumed that an ion which had been separated from a conducting surface by a distance equivalent to a number of atomic diameters was still weakly bound to the surface by an "electric image" force, of magnitude $e^2/(2x)^2$ dynes if the charge was e statcoulombs and the distance from the surface x cm. An external field E directed outward would tend to oppose this force, and the ion would be free when the net force dropped to zero. This would occur at a distance from the surface given by the relation

$$eE = e^2/(2x')^2 \qquad (12)$$

or

$$x' = \frac{1}{2}\left(\frac{e}{E}\right)^{1/2} \quad . \qquad (13)$$

In the present problem, the minimum value of x' would be 115 Å. The electrostatic potentials associated with the above forces are shown in Fig. 9. The potential difference $-e/4x$, measured from the potential of the surface, corresponds to the image force, whereas -Ex corresponds to the applied field. The combined potential would have a maximum at x = x', where its value would be $(eE)^{1/2}$ statvolts below that at the surface. Accordingly, the rate of emission would be increased by the factor

$$\exp\,[e(eE)^{1/2}/kT] \quad ,$$

in which k is Boltzmann's constant and T is the absolute temperature. This might be represented by straight lines on Fig. 7, with the ion current increasing in the range from 0 to 1800 volts by a factor of 2.12 at 680°C and of 2.16 at 655°C. The upper part of the experimental curve at 680°C has less slope than calculated, whereas the 655°C curve has more.

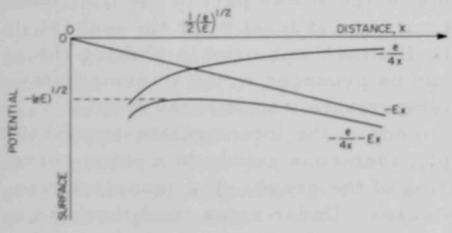

Fig. 9. Effect of an external electric field E upon the potential barrier overcome by an ion emitted from the conducting surface (Schottky effect). Electrical quantities are to be measured in absolute electrostatic units, distance in cm.

4. Effect of Filament Temperature

The effect of filament temperature in the closed-vessel unit (see Fig. 3) has already been touched upon in the above discussion. For convenience in the discussion, Fig. 8, obtained at a collecting potential of 130 volts has been divided into 3 regions which have been labelled "high-temperature region," "intermediate-temperature region," and "low-temperature region."

In the high-temperature region the ion currents varied with boat temperature (compare with Fig. 5), but not with filament temperature, nor with time, except for a warm-up period after the equipment had been off for some time. When the boat current was turned off, the ion current dropped very quickly to its boat-off value.

On the other hand, in the low-temperature region, the ion current tended to be of a transient nature, approaching equilibrium values which depended upon the filament temperature, but not upon the boat temperature. Recoverable ionizable material was stored, as discussed in the section on Effect of Collecting Potential at Low Filament Temperature.

In the intermediate-temperature region, the ion current depended upon both the boat temperature and the filament temperature. Possibly different mechanisms predominated at different points on the filament, since the temperature varied along the length, due to convection cooling and conduction toward the ends. However, the temperature spans covered by the curved portions of Fig. 8 were greater than the maximum temperature differences between points on the active part of the filament, by factors of at least 2 for the lowest curve to at least 5 for the highest. The temperature of the midpoint of the filament was used in plotting the curves. Striking transient effects could be produced in the intermediate-temperature region. If the filament temperature was lowered from a value in the high-temperature region to one in the intermediate-temperature region, the ion current dropped sharply, then rose slowly to a value corresponding to a point on the curved portion of the graph. The transient rise lasted for more than an hour in some cases. Under some conditions the ion current increased by a factor greater than 10. Recoverably ionizable material was deposited upon the filament during the ion current increase and also afterward.

5. Practical Significance of Ionization and Collection Effects

When quantitative measurements of chlorine-bearing gases are attempted by positive-ion-emission methods, 2 prominent difficulties are the lack of reversibility and of reproducibility.[13] The modified commercial equipment used in making the field tests gave a reproducible linear response so long as the concentration of Freon did not exceed 10 ppm.[1] If more was used, the response was nonlinear and the subsequent

return to the value for zero concentration was slow. In several new commercial units which were tested, the useful range for quantitative measurements was even less than from 0 to 10 ppm. The results just discussed indicate how it might be possible to extend the range of usefulness of the positive-ion-measuring method.

The products of high-temperature thermal decomposition of Freon produce an increase in the rate of release of alkali from the surface of a heated alkali compound such as the carbonate. This has been demonstrated in combustion furnace tests and also in flame tests. Quantitative rate-of-release tests using chlorine have been discussed above. The introduction of Freon has an effect similar to an increase in boat temperature, with all other variables held constant. It has not been established whether this is the only effect of Freon.

A surface covering the model discussed previously (see Fig. 4) would be a 3-dimensional graph of the ion current as a function of the filament temperature and collecting potential for one rate of supply of ionizable material, that corresponding to a boat temperature of 555°C. Similar models might have been constructed for other rates of supply if more extensive data had been obtained. However, it is not necessary to complete more models in order to show the relation between them, since Figs. 6 and 8 picture cross sections of a number of such models. A change in the rate of supply of ionizable material would produce a nontransient, reversible change in ion current only if the filament temperature and the collecting potential were each high enough so that the ion-current values, before and after the change, both fell upon the plateaus of the 3-dimensional graphs corresponding to the 2 rates of supply. It is necessary to fulfill this condition in order to make quantitative measurements. To provide a long, useful concentration range, the filament temperature should be as high as possible, the collecting potential as high as possible without danger of gaseous breakdown, and the rate of supply of alkali as low as possible. Ion currents exceeding the useful range should be avoided, if possible, or, as a relatively poor second choice, stopped quickly after they appear. The geometrical arrangement of the electrodes should be so arranged that the gas makes good contact with the source of ionizable material and the material from this source is spread over a large area of the ionizing surface.

The modified commercial detector used for field tests had been operated so as to satisfy some of the above requirements. The sensitive unit had been operated for a very long time, so that its background was very low, even at high temperature. Also, both the temperature and the collecting potential were maintained at relatively high values. However, the mechanism of the commercial unit is complicated by the fact that the collector is heated, so that ions which have been collected may be released subsequently as neutral particles and then possibly be ionized again.

6. The Effect of Various Gases upon Ionization and Collection

For the practical application of the positive-ion-emission method to atmospheric diffusion studies, the gases of interest are the normal constituents of the atmosphere at the test site, the tracer gas, and any other additives, such as the hydrogen used in the published field tests.[1] For studies of the mechanisms of operation of the measuring device, any gas is of interest if it affects the operation.

The effects of gases singly and in combination have been only partially investigated. The following have been used sometimes as the principal or carrier gas, at other times as an additive: air, nitrogen, oxygen, carbon dioxide, hydrogen, helium, and argon. Gases used only as additives include water vapor, methane, propane, butane, and ethyl alcohol, beside trace quantities of halogen-bearing gases. The carrier gas in a positive-ion apparatus serves as a transfer medium, and in addition some of its components may enter into reactions with gases or solids. The effects of the transport properties of the gas are reproducible and are reasonably simple in principle, although, as noted above, they may be quite difficult to describe with equations. The effects of the reactive or chemical properties have been found to be much more difficult to evaluate.

It was observed during the earliest studies with the commercial-type detector that water vapor and hydrogen could affect the ion current. In order to make measurements upon atmospheric samples without interference from water vapor, a cold trap was used which would pass Freon-12 but would reduce the concentration of water vapor to a very low level. The mechanism through which water vapor affects the ion current is not known with certainty. However, it has been established that the potassium carbonate-containing boat in the closed-vessel type of equipment can take on water vapor when cool and release some of it when heated. Unless it is heated extremely slowly, the salt may decompose explosively and contaminate the filament with fragments.

With the commercial-type sensitive element, 3 or 4% hydrogen added to the air stream lowered somewhat the background ion current and also the ion current due to Freon, but it increased the stability of operation. The mechanism is not completely understood. At least part of the hydrogen was burned in the detector, so that the exhaust gas was moist even though the entering gas was dry.

When the noble gases argon and helium and the relative stable gas nitrogen were each used alone in the closed-vessel-type unit, and when helium and nitrogen were used as additives to argon, the background ion-current effects associated with change in gas composition were essentially immediate, reproducible, and reversible. The difference between argon

and helium was attributed to the difference in their physical properties. Nitrogen also seemed to be a nonreactive medium. In retrospect, it appears to be very improbable that the effects of residual air, of oxygen in particular, were ever completely removed from the apparatus during these tests, in spite of a gas-preparation train and of repeated pumping and refilling of the reaction vessel. To remove oxygen completely, it might be necessary to build a system that could be baked out and to provide a gettering device inside the enclosure.

Large background ion-current effects could be produced by the use of small amounts of hydrogen and oxygen, singly and in combination, in an atmosphere of argon that had been passed through a purifying train consisting of a solid carbon dioxide-alcohol trap (-78°C) for water and hydrocarbons, hot copper (about 700°C) for oxygen, hot cupric oxide (about 700°C) for hydrogen and carbon monoxide, "Ascarite" (a sodium hydroxide preparation) for carbon dioxide, and a second solid carbon dioxide-alcohol trap and a magnesium perchlorate trap for water passed by the first or produced later, and finally hot magnesium pieces in a stainless steel tube (about 700°C) for nitrogen. The results of several type of manipulation are presented in Fig. 10 and its legend.

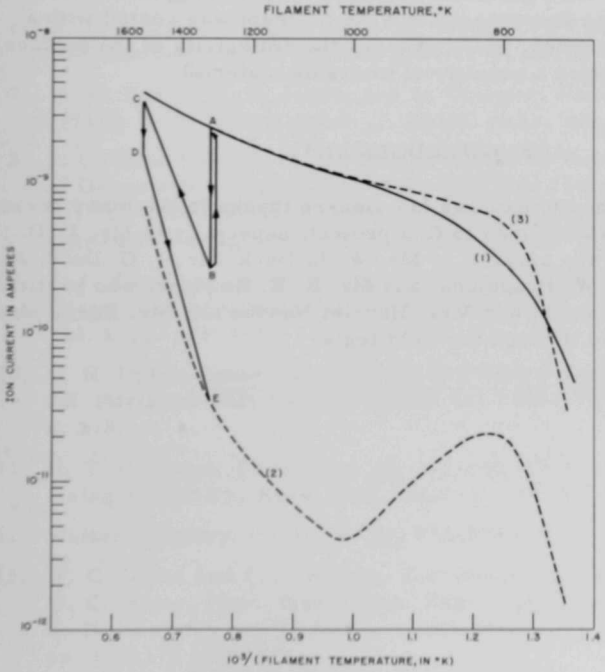

Fig. 10

Positive ion current as a function of filament temperature, additives, and time. Curve (1) represents average of data after long runs (16 to 64 hr) in argon plus 0.33% hydrogen. Curve (2) was obtained after refilling with argon + 0.33% hydrogen and using the "flashing" procedure indicated by ABCDE, with AB and CD representing the effect of time, BC and DE the effect of temperature. Curve (3) shows the effect of adding a trace of oxygen to argon plus 0.33% by hydrogen while conditions corresponded to Curve (2).

Apparently these gases entered into reactions in the bell, combining chemically with other gases or with solids. There seem to be at least 2 separate hydrogen effects, one associated with the filament (flashing, see Fig. 10) and the other associated with the boat (a reduction in the degree of carry-over of the chlorine effect after the gaseous chlorine had been removed).

Atmospheric air may contain traces of organic gases. Propane (C_3H_8) to the extent of 100 ppm in argon was found to produce marked changes of the filament. After a few hours, the filament developed an uneven, spotty appearance as viewed through an optical pyrometer with red light (6500 Å). At the same time, there was an increase in the amount of power required to maintain the filament resistance at a constant value. If the filament was turned off and observed at room temperature, it appeared to be dull or dark when viewed directly or at low magnification. The pattern of the variations of ion current with filament temperature, collecting potential, and boat temperature suggested that some ionizable material had been deposited upon the filament. These changes could be prevented by using an excess (0.33%) of oxygen along with the propane. Less extensive tests were made with other organic compounds. Butane (C_4H_{10}) and ethyl alcohol (C_2H_5OH) appeared to be similar in action to propane, but methane (CH_4) had little or no effect. As a plausible explanation, it is suggested that the organic compounds were decomposed and the filament was coated with a nonuniform deposit of carbon, which changed the emissivity of the surface, and which possibly trapped a quantity of ionizable material.

ACKNOWLEDGEMENT

The author wishes to express his sincere thanks to the many persons who contributed efforts and ideas to this project, especially to Mr. L. D. Marinelli who initiated the project, to Mr. W. L. Buck, Mr. J. G. Dodd, Jr., Mr. R. H. Hussey, Mr. W. Prepejchal and Mr. R. E. Rowland, who participated in the laboratory work, and Mrs. Harriet Newton and Mr. Harry Moses, who planned and carried through the field tests.

REFERENCES

1. H. Moses, Fourth Atomic Energy Commission Air Cleaning Conference, Argonne National Laboratory, November 1955 (Div. of Reactor Development, Washington, D.C., 1956) TID-7513, Pt. 1, pp. 177-85; H. A. Schultz, Anal. Chem. 20, 1840-1842 (1957).

2. J. F. Miller, H. Hart and E. L. McBee, Ind. Eng. Chem., Anal. Ed. 19, 148-149 (1947); R. H. Kimball and L. E. Tufts, ibid., 19, 150-153 (1947); P. J. Elving and W. B. Ligett, ibid., 14, 449-453 (1942); M. L. Nichols and J. S. Olsen, ibid., 15, 342-346 (1943).

3. E. Biesalki, Z. angew. Chem. 37, 314-317 (1924).

4. Fluid Motion Panel of the Aeronautical Research Committee and others, Modern Developments in Fluid Dynamics, S. Goldstein, Ed. (Oxford University Press, London, EC 4, 1938) Vol. II, pp. 641-643; Modern Developments in Fluid Dynamics, High Speed Flow, H. B. Squire, Ed. (Oxford University Press, London, EC 4, 1953) Vol. II, pp. 806-810.

5. Y. S. Touloukian, G. A. Hawkins, and M. Jakob, Trans. Am. Soc. Mech. Engrs. 70, 13-18 (1948); M. Jakob, Heat Transfer (John Wiley and Sons, Inc., New York, 1949) Vol. I, p. 530.

6. H. A. Schultz, Argonne National Laboratory Radiological Physics Division Semiannual Report, ANL-5755, pp. 22-28 (1957).

7. W. H. Furry, R. C. Jones, and L. Onsager, Phys. Rev. 55, 1083-1095 (1939); W. H. Furry and R. C. Jones, Phys. Rev. 69, 459-471 (1946).

8. J. O. Hirschfelder, C. F. Curtiss and R. B. Bird, Molecular Theory of Gases and Liquids (John Wiley and Sons, Inc., New York, 1954) pp. 523-582; Ludwig Waldmann, Handbuch der Physik, S. Flugge, Ed. (Springer Verlag, Berlin, 1958) Vol. XII, pp. 396-400, 428-429.

9. J. J. Thomson and G. P. Thomson, Conduction of Electricity through Gases (Cambridge University Press, London, 1928) Third edition, Vol. I, pp. 375-381.

10. G. H. Dieke, American Institute of Physics Handbook, Dwight E. Gray, Ed. (McGraw-Hill Book Company, Inc., New York 1957) Section 7, p. 218.

11. K. T. Compton, Phys. Rev. 22, 333-346 (1923); K. T. Compton and Irving Langmuir, Revs. Mod. Phys. 2, 219-221 (1930).

12. Walter Schottky, Physik Z. 15, 872-878 (1914).

13. W. C. White and J. J. Hickey, Electronics 21, 100-102 (March 1948); W. C. White, Proc. Inst. Radio. Engrs. 38, 852-858 (1950); H. A. Schultz, R. E. Rowland, and L. D. Marinelli, Quarterly Report, ANL-4531, pp. 169-176 (1950).

APPENDIX

THEORY OF NATURAL CONVECTION NEAR A SINGLE VERTICAL FILAMENT AT HIGH TEMPERATURE

The approximate theory of convection derived below has been applied in the body of the report to provide semiquantitative explanations of the effects of the physical properties of the carrier gas upon the observed ion currents and rates of heat loss. The general equations are not integrable into closed forms by standard procedures, but 2 special cases, those of a "thin film" and "thick film," are easy to handle. The derivation is based upon the boundary-layer concept introduced by Prandtl and developed by Kramer, Frankl, and others. The steps of the development are similar to those used to obtain a published theory of a heated vertical plate.[1,2] The calculated rates of heat loss are somewhat more than one-half the experimental rates, in both thin-film and thick-film examples. It is suggested that this is due, at least in part, to the inadequacy of the functions which were chosen to represent the temperature and velocity distributions along a perpendicular to the heated surface.

General Case

Because of the symmetry around the axis of the vertical wire, the problem was set up in cylindrical coordinates, with the positive Z axis oriented vertically upward. As in the corresponding theory for a flat vertical plate, 2 horizontal planes were drawn an infinitesimal distance apart and attention was fixed upon the fluid enclosed between these planes (see Fig. A1). The time rate of change of vertical momentum was equated to the applied vertical forces (buoyant and viscous forces). The heat flowing into this section by thermal conduction in a horizontal direction was equated to the heat flowing out by mass motion in a vertical direction, neglecting internal heating due to the viscosity of the gas. It was assumed, as is usual in boundary-layer theories, that the vertical component of the gas velocity dropped to zero and the temperature dropped to its constant static value at a finite radial distance from the wire, r = R(z) (a function of z), and that the horizontal gradients of the 2 variables vanished. To be rigorous, it would be necessary to allow these quantities to approach zero asymptotically as r approached infinity, but from the practical standpoint, they may be neglected beyond a certain finite R.

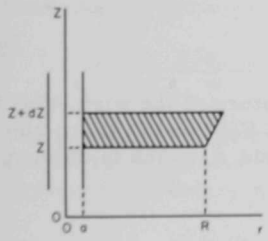

Fig. A1

Cross section of volume element considered in equations 1, and 2.

The equations for momentum and energy are, respectively:

$$\frac{\partial}{\partial z}\int_a^R \rho u^2\, 2\pi r\, dr = g\int_a^R (\rho_0 - \rho) 2\pi r\, dr - 2\pi a \left(\eta \frac{\partial \mu}{\partial r}\right)_{r=a} \quad (1)$$

and

$$\frac{\partial}{\partial z}\int_a^R \rho u C_p (T - T_0)\, 2\pi r\, dr = -2\pi a \left(k \frac{\partial T}{\partial r}\right)_{r=a} , \qquad (2)$$

where the common factor 2π has been retained to indicate that $2\pi r\, dr$ is an element of area. The variables ρ and T represent the local density of the gas and the absolute temperature, respectively, whereas ρ_0 and T_0 denote the values a long distance from the filament. The remaining variable, u, is the vertical component of the velocity. The constants are g, the acceleration of gravity, C_p, the specific heat at constant pressure (independent of the temperature in the cases studied), η, the viscosity, and k, the thermal conductivity. The lower limit a is the radius of the wire. In deriving these equations, the procedure was analogous to that in the flat-plate case, except that it was not assumed[3] that $(\rho_0 - \rho)$ was much less than ρ_0, or that $(\rho_0 - \rho)/(T - T_0)$ was a constant, or[4] that $T - T_0$ was much less than T_0. In fact, $(T - T_0)/T_0$ was to vary from zero to 3.33 in the region near the ionization filament. In view of this, the relation between density and temperature was expressed by Charles' Law:

$$\rho T = \rho_0 T_0 , \qquad (3)$$

which was valid because the difference in pressure between the 2 ends of the wire was negligible relative to atmospheric pressure. It should be noted that, due to the conservation of mass, the radial component of the velocity could not possibly vanish all along the surface defined by r = R(z).

The next step was to assume that the distributions of density and vertical velocity component could be represented by

$$\rho_0 - \rho = (\rho_0 - \rho_1)F(\xi) \qquad (4)$$

and

$$u = U(z)G(\xi) , \qquad (5)$$

in which ρ_1 is the density of the gas at the temperature of the wire, U(z) is a proportionality factor depending upon z only, and $F(\xi)$ and $G(\xi)$ are functions of r only, expressed in terms of a new variable ξ, which is defined by the relation

$$\xi = \frac{R - r}{R - a} . \qquad (6)$$

This variable ξ varies from zero at the outer edge of the boundary layer (r = R) to unity at the surface of the wire (r = a). See Fig. A2. The

functions $F(\xi)$ and $G(\xi)$ and their first derivatives must all vanish at the outer edge of the boundary layer ($\xi = 0$) to satisfy the assumptions made in deriving the differential equations. The value of $F(\xi)$ at the wire ($\xi = 1$) must be unity, and $G(\xi)$ must vanish, since the value of ρ is ρ_1 there and it is assumed that there is no slip. These properties are summarized as follows:

$$F(0) = 0 \quad ; \quad F'(0) = 0 \quad ; \quad F(1) = 1$$
$$G(0) = 0 \quad ; \quad G'(0) = 0 \quad ; \quad G(1) = 0 \quad . \tag{7}$$

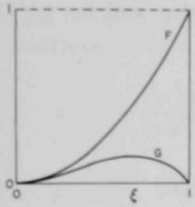

Fig. A2

Particular temperature and velocity distribution functions F and G in terms of the dimensionless variable $\xi = R\text{-}r/R\text{-}a$. Equations are $F(\xi) = \xi^2$ and $G(\xi) = \xi^2(1 - \xi)$.

The assumption that a single $F(\xi)$ and a single $G(\xi)$ are adequate to describe the density and velocity distributions at all values of z is probably one of the weaker parts of the theory. There is experimental evidence for the similar assumption made for the case of the plane wall, with the temperature difference between the wall and the gas, $T_1 - T_0$, much less than the initial absolute temperature of the gas, T_0.

The density and velocity distribution functions defined above equations (4,5) were substituted into the momentum and energy equations (1,2), and the running variable was changed from r to ξ. The product r dr was replaced by its equivalent

$$r\,dr = -a^2\delta[\delta(1 - \xi) + 1]\,d\xi \tag{8}$$

involving the dimensionless variable δ, defined by the equation

$$\delta(z) = \frac{R(z) - a}{a} \quad . \tag{9}$$

The limits of the integrals were changed correspondingly. The momentum and energy equations (1,2) were thus reduced to the following system of first-order ordinary differential equations:

$$a^2 \frac{d}{dz} U^2 \delta(K_3\delta + L_3) = g \frac{\rho_0 - \rho_1}{\rho_0} a^2 \delta(K_1\delta + L_1) + \frac{\rho_1 \nu_1}{\rho_0} G'(1) \frac{U}{\delta} \tag{10}$$

$$a^2 \frac{d}{dz} U\delta (K_2\delta + L_2) = \frac{\rho_0}{\rho_1} \alpha_1 \frac{F'(1)}{\delta} \quad , \tag{11}$$

in which ν_1 is the value of the kinematic viscosity:

$$\nu = \eta/\rho \tag{12}$$

at the temperature of the wire, α_1 is the value of the thermal diffusivity:

$$\alpha = k/C_p\rho \tag{13}$$

at the same temperature, and the 6 positive constants K_i, and L_i, i = 1,2,3, are the values of the integrals

$$K_i = \int_0^1 (1 - \xi)\, H_i(\xi) d\xi \quad ; \quad L_i = \int_0^1 H_i(\xi) d\xi$$

$$H_1(\xi) = F(\xi) \qquad H_2(\xi) = F(\xi)G(\xi) \tag{14}$$

$$H_3(\xi) = [1 - \frac{\rho_0 - \rho_1}{\rho_0} F(\xi)][G(\xi)]^2 \quad .$$

Two Special Cases

The 2 ordinary differential equations (10,11) are more complicated than those derived for the plane-wall case because of the presence of the terms involving K_1, K_2, and K_3. Consequently, it does not appear to be possible to obtain a general solution in a closed form. However, in case the constants K_1, K_2, and K_3 may be neglected relative to L_1, L_2, and L_3, respectively, the equations take the same form as in the case of the plane wall, and therefore they lead to the same type of solution. This "thin-film" solution is applicable in case the cylinder has a relatively large radius, or in case the temperature difference is small. However, under the conditions of the high-temperature ionization experiments in argon and helium, the relations

$$\text{(Thin)} \quad \delta << K_i/L_i \quad ; \quad i = 1,2,3$$

were satisfied only at the extreme lower end of the filament. This suggested that a useful approximate "thick-film" theory might be obtained by making the alternate assumption:

$$\text{(Thick)} \quad K_i/L_i << \delta \quad ; \quad i = 1,2,3$$

The same method of integration may be used for both special cases, thin film and thick film. Since z does not appear explicitly in the general differential equations (10,11), an equation relating only U and δ may be

obtained by eliminating dz. The general U, δ differential equation has the form of Abel's equation of the second kind.(5) Either of the 2 approximations to this equation may be integrated by use of an integrating factor of the form $U^p \delta^q$, in which p and q are constant exponents, different in the 2 cases. The solutions are

$$\text{Thin:} \quad U^{5+3\lambda'} \delta^{3+3\lambda'} \left[U - \frac{\mu'}{\lambda' + (5/3)} \delta^2 \right] = \text{constant} \tag{15}$$

$$\text{Thick:} \quad U^{4+(5\lambda/2)} \delta^{5+5\lambda} \left[U - \frac{\mu}{\lambda + (8/5)} \delta^3 \right] = \text{constant} \quad , \tag{16}$$

in which λ and μ are positive constants representing combinations of the coefficients in the differential equations:

$$\lambda = \frac{\nu_1}{\alpha_1} \left(\frac{\rho_1}{\rho_0} \right)^2 \left(\frac{-G'(1)}{F'(1)} \right)$$

$$\mu = \frac{ga^2}{\alpha_1} \frac{\rho_1(\rho_0 - \rho_1)}{\rho_0^2} \frac{1}{F'(1)} \frac{K_1 K_2}{K_3} \quad , \tag{17}$$

and λ' and μ' are similar positive constants with each K replaced by the corresponding L. (The constants λ and λ' are dimensionless, whereas μ and μ' have the dimensions of velocity.)

There is considerable similarity between the 2 families of solutions, (15) and (16), in the region of interest, namely, the first quadrant of the U, δ plane (see Fig. A3). If the constant of integration is positive, U approaches infinity as δ approaches zero. If the constant is negative, δ approaches infinity as U approaches zero. Only if the constant of integration is zero can U approach zero as δ approaches zero. The origin is a singular point in both special cases, also in the general case. Both axes U = 0 and δ = 0 satisfy the U, δ differential equations.

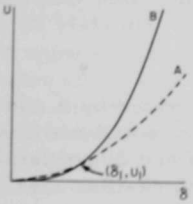

Fig. A3

Asymptotes approached by U, δ relation.

A, thin film, for small δ, $U = [C_1'/(C_2')^2]\delta^2$

B, thick film, for large δ, $U = (C_1/C_2^3)\delta^3$

In the thin-film case, if the boundary conditions are chosen to be the same as in the plane-wall case:

$$\text{Thin:} \quad U = 0, \quad \delta = 0 \quad \text{at } z = 0 \quad , \tag{18}$$

then the parabola

$$\text{Thin:} \quad U = \frac{\mu'}{\lambda' + (5/3)} \delta^2 \tag{19}$$

is the only solution which is physically significant. If this relation is substituted into the thin-film approximation of the second of the ordinary differential equations (11), the resulting equation may be integrated at once to obtain

$$\text{Thin:} \quad U = C_1' (z - z_0')^{1/2} \quad ; \quad \delta = C_2' (z - z_0')^{1/4} \quad , \tag{20}$$

in which the constants C_1' and C_2' are combinations of the coefficients of the differential equations and z_0' is a constant of integration, which must be set equal to zero to satisfy the thin-film boundary conditions (18).

The thick-film case is applicable only for large δ, great relative to L_i/K_i, i = 1,2,3. Accordingly, the constant of integration in (16) need not be restricted to zero. The first quadrant of the U, δ plane is divided into 2 regions by the cubic (see Fig. A3)

$$U = \frac{\mu}{\lambda + (8/5)} \delta^3 \quad . \tag{21}$$

If the constant of integration is positive, the integral curve lies within the region bounded by the U axis and the cubic, and approaches both these boundaries asymptotically with increasing U. If the constant of integration is negative, the corresponding integral curve lies on the other side of the cubic, in the region bounded by the cubic and the δ axis, and approaches these boundaries asymptotically with increasing δ. Accordingly, all possible physically significant portions of the solution (16) approach the cubic (21) from one side or the other as U and δ both become large. For any given curve of the family, the U deviations from the cubic vary approximately as δ^{-17} or $U^{-(17/3)}$, and the δ deviations approximately as δ^{-19} or $U^{-(19/3)}$ for $\lambda \ll 1$ as in the ionization experiments.

The parabola (19) and the cubic (21) represented by A and B of Fig. A3 are asymptotes approached at U and δ very small and U and δ very large, respectively. The corresponding U, z and δ, z relations are: in the thin-film case, equations (20); in the thick-film case,

$$U = C_1 (z - z_0)^{1/2} \quad ; \quad \delta = C_2 (z - z_0)^{1/6} \quad , \tag{22}$$

in which C_1 and C_2 are combinations of the coefficients of the 2 thick-film equations and z_0 is a constant of integration, yet to be evaluated.

To determine whether or not the asymptotic thick-film solution (21,22) will be useful in a particular problem, it is necessary to evaluate the various constants numerically. The constants C_1, C_2, C_1', and C_2' were introduced above to represent combinations of the constants of the differential equations:

$$\text{Thin:} \quad (C_1')^2 = g \frac{\rho_0(\rho_0 - \rho_1)}{\rho_1^2} \frac{4L_1F'(1)}{3L_2[-G'(1)]} \frac{1}{N'}$$

$$(C_2')^4 = \frac{\alpha_1^2}{ga^4} \frac{\rho_0}{\rho_0 - \rho_1} \frac{4}{3} \frac{F'(1)[-G'(1)]}{L_1L_2} N' \tag{23}$$

$$N' = \frac{\nu_1}{\alpha_1} + \left(\frac{\rho_0}{\rho_1}\right)^2 \frac{5}{3} \frac{L_3F'(1)}{L_2[-G'(1)]}$$

$$\text{Thick:} \quad C_1^2 = g \frac{\rho_0(\rho_0 - \rho_1)}{\rho_1^2} \frac{6K_1F'(1)}{5K_2[-G'(1)]} \frac{1}{N}$$

$$C_2^6 = \frac{\alpha_1^2}{ga^4} \frac{\rho_0}{\rho_0 - \rho_1} \frac{6}{5} \frac{F'(1)[-G'(1)]}{K_1K_2} N \tag{24}$$

$$N = \frac{\nu_1}{\alpha_1} + \left(\frac{\rho_0}{\rho_1}\right)^2 \frac{8}{5} \frac{K_3F'(1)}{K_2[-G'(1)]} .$$

In these equations ρ_1/ρ_0 and $(\rho_0 - \rho_1)/\rho_0$ depend only upon the temperature conditions of the problem. The values of $F'(1)$, $G'(1)$, K_1, K_2, L_1, and L_2 depend only upon the functions F and G chosen to represent the radial density and velocity distributions. The values of K_3 and L_3 depend upon both the temperature conditions and the radial distribution functions. Only the diffusivity α_1 and the kinematic viscosity ν_1 depend upon the particular gas used.

Application to Ionization Experiments

To approximate the conditions of the ionization experiments, the temperatures of the gas and the filament were taken as $T_0 = 300°K$ and $T_1 = 1300°K$, respectively, and the corresponding density ratios became $\rho_0/\rho_1 = \frac{13}{3}$ and $(\rho_0 - \rho_1)/\rho_1 = \frac{10}{13}$. The radius a of the wire was 0.015 cm. The value of the diffusivity at the temperature of the filament was taken as $\alpha_1 = 19.88$ cm^2/sec for helium and as 2.52 for argon, based on conductivities computed for 1300°K by the use of room-temperature values and classical collision theory, assuming Lennard-Jones intermolecular potential functions.(6) The Prandtl number ν_1/α_1 was taken as $\frac{2}{3}$, the value of classical collision theory for monatomic gases.

The simplest polynomials which satisfy the conditions (7) required of $F(\xi)$ and $G(\xi)$ at $\xi = 0$ and $\xi = 1$ are (see Fig. A2).

$$F(\xi) = \xi^2 \quad ; \quad G(\xi) = \xi^2(1 - \xi) \quad , \tag{25}$$

in which case

$$F'(1) = 2 \quad ; \quad K_1 = 1/12 \quad ; \quad K_2 = 1/105 \quad ; \quad K_3 = 2.655 \times 10^{-3}$$

$$-G'(1) = 1 \quad ; \quad L_1 = 1/3 \quad ; \quad L_2 = 1/30 \quad ; \quad L_3 = 6.471 \times 10^{-3} \; . \tag{26}$$

The constants of the asymptotic thick-film and the thin-film solutions turn out to be:

Thick	Thin
$N = 17.42$	$N' = 12.82$
$C_1 = 130.6 \text{ cm}^{1/2}/\text{sec}$	$C_1' = 171.6 \text{ cm}^{1/2}/\text{sec}$
He: $C_2 = 90.39 \text{ cm}^{-1/6}$	He: $C_2' = 422.5 \text{ cm}^{-1/4}$
A: $C_2 = 45.4 \text{ cm}^{-1/6}$	A: $C_2' = 150 \text{ cm}^{-1/4}$

It is to be noted that N and N' are much larger than ν_1/α_1, so that if the viscous forces at the surface of the wire were neglected relative to the inertial forces (by setting $\nu_1 = 0$), N and N' would be decreased by only 4 and 5%, respectively, C_1 and C_1' would be increased by about 2%, and C_2 and C_2' decreased by about 1%.

The coordinates U_1, δ_1 of the intersection of the quadratic and cubic U, δ relations (see Fig. A3), and the corresponding vertical distance z_1' determined by the thin-film relation (20) are:

Helium	Argon
$\delta_1 = 5.404$	$\delta_1 = 5.404$
$U_1 = 2.806 \times 10^{-2} \text{ cm/sec}$	$U_1 = 2.214 \times 10^{-1} \text{ cm/sec}$
$z_1' = 2.677 \times 10^{-8} \text{ cm}$	$z_1' = 1.67 \times 10^{-6} \text{ cm}$

The value of δ_1 is somewhat greater than $L_1/K_1 = 4$, $L_2/K_2 = 3.5$, and $L_3/K_3 = 2.430$. The values of z_1' are so small relative to the length of the wire, L = 8.1 cm, that it is reasonable to neglect the starting section completely in considering the conditions near the upper end of the wire and to use the cubic U, δ relation (21) and the corresponding z equations (22) with $z_0 = 0$. To check on the validity of this approximation, the general differential equations for argon were integrated by an approximate numerical

method, and the values of U and δ obtained for the top of the wire were about 1.5% lower than those given by the thick-film equations. As the calculated U, δ relation made the transition from quadratic to cubic, for values of U near U_1 (see Fig. A3), the values of δ dropped to 80% of the values given by the discontinuous curve made up of the quadratic and the cubic (see Fig. A3).

The rate of heat loss from the filament by convection will be equal to the rate at which heat is carried upward through a horizontal plane at the top of the filament, which is just the integral in the second of the original differential equations (2) evaluated at z = L = 8.1 cm:

$$P = J\int_a^R [\rho u C_p (T - T_0)]_{z=L}\, 2\pi r dr \quad . \tag{27}$$

The factor J, inserted here, may be used to convert from thermal to mechanical units. After eliminating T through use of Charles' Law (3) and transforming the variables as above, the power equation associated with the cubic U, δ relation reduces to

$$\text{Thick:} \quad P = J(2\pi C_p)(\rho_0 - \rho_1)\, T_0 a^2 K_2 [U\delta^2]_{z=L}$$

$$= J(2\pi C_p)(\rho_0 - \rho_1)\, T_0 a^2 K_2 C_1 C_2^2 L^{5/6} \quad . \tag{28}$$

Since argon and helium are both monatomic, each of the products $C_p \rho_0$ and $C_p \rho_1$ has the same value for both gases, provided the values of T_0 and T_1 are the same. Since C_1 is also independent of the gas, the power depends upon the gas only through the factor C_2^2, and therefore the power is proportional to $\alpha_1^{2/3} = (k_1/C_p \rho_1)^{2/3}$ and thus is proportional to $k_1^{2/3}$ (evaluated at T_1). Since the thermal conductivity of helium at the temperature of the filament is 7.89 times that of argon, the above equation indicates that the power losses by convection will be in the ratio of 3.96 to 1. It should be noted that this ratio does not depend at all upon the radial distribution functions $F(\xi)$ and $G(\xi)$ that are chosen, so long as the same are used for both gases.

Two other ratios are independent of the choice of the F and G functions. For a given altitude z the velocity functions U have identical values, and the film thicknesses δ vary as $\alpha_1^{1/3}$, so the film in helium turns out to be 1.99 times as thick as that in argon.

To calculate numerical values of P, U, and δ, it is necessary to choose specific functions $F(\xi)$ and $G(\xi)$. Using the functions mentioned above, (25), and the corresponding constants C_1, C_2, and N already calculated, the values in Table I were obtained.

Table I

THICK-FILM CALCULATIONS COMPARED WITH EXPERIMENT

	Helium	Argon
Power P, watts	16.1	4.07
Radius of disturbance R = a[δ(L) + 1], cm	1.93	0.98
Maximum velocity (4/27)U(L), cm/sec	55.7	55.7
Radius of velocity maximum a[δ(L)/3 + 1], cm	0.65	0.34
Maximum Reynolds number	12.2	65.0
Experimental		
Power, watts, total	34.6	10.7
Allowance, radiation and ends[a]	3.5	3.5
Net Convection	31.1	7.2

[a]Computed radiation rate, 1.5 watts. Estimated end losses, 2 watts. End losses in a vacuum, 3 watts, were used for the gaseous case in ANL-5755, but optical pyrometer measurements of the incandescent portion of the filament indicated that the temperature gradient near the ends was smaller in gases than in a vacuum.

The calculated power values are a little more than one-half the experimental values (52% for helium; 57% for argon). Possibly, the principal reason is that the arbitrary F and G functions constitute a less efficient combination than those which exist in experiments. The distributions produced by experiment will certainly be influenced by the dependence of viscosity and thermal conductivity upon temperature. Also, it is probable that F and G will vary with z. Several different combinations of F and G were tried, and some were found to be somewhat more effective in dissipating heat than the above parabolic F and cubic G.

Another source of error is the influence of the collectors and the upper guard ring, which is neglected in the above theory. Since these electrodes lie on a cylinder of 1.3-cm radius, they would be expected to affect the convection pattern in helium, at least near the top of the filament.

Application of the Thin-film Case

The thin-film theory was compared with the empirical relation given by Touloukian, Hawkins, and Jakob[7] to summarize their work with cylinders of 2.75-in. diameter and 6 to 36 in. in length, in water and ethylene glycol, with maximum temperature differences of 83.5°F. The rates of heat loss, calculated through the use of the specific F and G functions above (2,5), average 63% as great as given by the empirical relation (61% for water and 66% for ethylene glycol). Also, the calculated values of δ, the ratio

of the film thickness to the radius of the cylinder, are much less than the ratios L_i/K_i, i = 1,2,3, as they must be if the thin-film theory is to be applied.

To make the comparison, the thin-film theory was specialized for small temperature differences and for liquids, and the resulting relation for power loss was written in dimensionless form. In the theory as given above, only the original partial differential equations (1,2) are applicable to either gases or liquids. If the temperature differences are small, these 2 equations may be simplified somewhat by replacing ρ by ρ_0 except in the buoyancy term on the right-hand side of (1), where $\rho_0 - \rho$ is replaced by using the equation of expansion:

$$\frac{\rho_0 - \rho}{\rho_0} = \beta(T - T_0) \quad , \tag{29}$$

in which β is the coefficient of volumetric expansion (which may be set equal to $1/T_0$ in the case of a gas). Also, η and k are taken as constants, and in the case of a liquid C_p is replaced by the specific heat C. In view of the equation of expansion, $F(\xi)$ is redefined through

$$T - T_0 = (T_1 - T_0)F(\xi) \quad . \tag{30}$$

If the derivation is carried out as before, the results are the same as if the above substitutions were made in the final solutions and the temperature-dependent term $(\rho_0 - \rho_1)F(\xi)/\rho_0$ was dropped from the definition of K_3 and L_3. The theoretical thin-film heat-loss relation, in dimensionless form, is then

$$N_{Nu} = \left[\left(\frac{4}{3}\right)^3 \frac{L_1 L_2 F'(1)}{-G'(1)}\right]^{1/4} \left[\frac{g\beta(T_1 - T_0)L^3}{\nu^2}\right]^{1/4} \left[\frac{\nu}{\alpha}\right]^{1/2} \left[\frac{\nu}{\alpha} + \frac{5L_3 F'(1)}{3L_2[-G'(1)]}\right]^{-1/4} . \tag{31}$$

The Nusselt number

$$N_{Nu} = hL/k \tag{32}$$

is defined in terms of a new variable h, which is the surface coefficient of heat transfer, the average rate of heat loss per degree difference between the initial temperature of the fluid and the temperature of the surface. The first bracketed factor in (31) represents a proportionality constant, the second is the dimensionless Grashof number N_{Gr} (with L as characteristic dimension), and the third and fourth are functions of the dimensionless Prandtl number $N_{Pr} = \nu/\alpha$.

The above authors' empirical relation was

$$N_{Nu} = 0.726 \, (N_{Gr} \, N_{Pr})^{1/4} \quad . \tag{33}$$

The Prandtl numbers given in the paper are 2.43 for water and 117.77 for ethylene glycol. On the basis of the simple F and G functions (22) above, $L_3 = \frac{1}{105}$ when the density differences are small, and the second term in the last bracket of (31) has the value of 0.952. In this case the viscous forces are more important than the inertial forces, exactly opposite to the case of the fine wire at high temperature in gas. The product of the last 2 brackets of (31) deviates from 0.959 $(\nu/\alpha)^{1/4}$ by only 4.1% at each of the above 2 values of ν/α. If these 2 brackets are replaced by this approximate value, equation (31) takes the form of the empirical relation (33), with the numerical constant replaced by

$$\left[\left(\frac{4}{3}\right)^3 \frac{L_1 L_2 F'(1)}{-G'(1)}\right]^{1/4} (0.959) = 0.460 \quad , \tag{34}$$

which is 63.4% of the empirical value 0.726. Calculated values of δ are all less than 0.22, which satisfies the condition that δ must be small relative to $L_1/K_1 = 4$, $L_2/K_2 = 3.5$, and $L_3/K_3 = 2.67$.

REFERENCES

1. E. R. G. Eckert and R. M. Drake, Jr., Heat and Mass Transfer (McGraw-Hill Book Company, Inc., New York, 1959) Second Edition, pp. 131-134, 167-169, 312-317.

2. H. B. Squire, Modern Developments in Fluid Dynamics, High Speed Flow, L. Howarth, Ed. (Oxford University Press, London, EC 4, 1953) Vol. II, pp. 770-773, 806-810.

3. Eckert and Drake, op. cit., p. 235.

4. H. B. Squire, op. cit., p. 809.

5. E. Kamke, Differential Gleichungen, Loesungsmethoden und Loesungen, (Akademische Verlagsgesellschaft Becker u. Erler, Kom.-Ges., Leipzig, Reprinted by Chelsea Publishing Co., 231 W. 29th Street, New York, 1948) Third Edition, Vol. I, pp. 26-28.

6. J. E. Lennard-Jones, Proc. Roy. Soc. (London) A106, 463-477 (1924); J. O. Hirschfelder, C. F. Curtis, and R. B. Bird, Molecular Theory of Gases and Liquids (John Wiley and Sons, Inc., New York 1954) p. 162.

7. Y. S. Touloukian, G. A. Hawkins, and M. Jakob, Trans. Am. Soc. Mech. Engrs. 70, 13-18 (1948).